Dalton Transactions

Benchmarking the dynamic luminescent properties and UV stability of B18H22-based materials

Journal:	*Dalton Transactions*
Manuscript ID	DT-COM-04-2022-001225.R1
Article Type:	Communication
Date Submitted by the Author:	18-May-2022
Complete List of Authors:	Anderson, Kierstyn; UCLA, Chemistry and Biochemistry Hua, Ash; UCLA, Chemistry and Biochemistry Plumley, John; Air Force Research Laboratory, Space Vehicles Directorate Ready, Austin; UCLA, Chemistry and Biochemistry Rheingold, Arnold; University of California, Department of Chemistry and Biochemistry Peng, Thomas; Air Force Research Laboratory, Space Vehicles Directorate Djurovich, Peter; University of Southern California, USC Chemistry Department Kerestes, Christopher; Air Force Research Laboratory, Space Vehicles Directorate Snyder, Neil; BlueHalo Andrews, Andrew; BlueHalo Caram, Justin; UCLA Division of Physical Sciences, Chemistry and Biochemisry; Dr. Spokoyny, Alex; UCLA, Chemistry and Biochemistry

ARTICLE

Benchmarking the dynamic luminescent properties and UV stability of $B_{18}H_{22}$-based materials

Received 00th January 20xx,
Accepted 00th January 20xx

DOI: 10.1039/x0xx00000x

Kierstyn P. Anderson,[a] Ash Sueh Hua,[a] John B. Plumley,[b,c] Austin D. Ready,[a] Arnold L. Rheingold,[d] Thomas L. Peng,[b] Peter I. Djurovich,[e] Christopher Kerestes,[b] Neil A. Snyder,[f] Andrew Andrews,[f] Justin R. Caram,[a]* and Alexander M. Spokoyny[a]*

The dynamic photoluminescent properties, and potential quenching mechanisms, of *anti*-$B_{18}H_{22}$, 4,4'-Br_2-*anti*-$B_{18}H_{20}$, and 4,4'-I_2-*anti*-$B_{18}H_{20}$ are investigated in solution and polymer films. UV stability studies of the neat powders show no decomposition occurring after intense 7 day light soaking. In contrast, clusters incorporated into polymer films are found to degrade into smaller borane fragments under the same irradiation conditions. To highlight the utility of these compounds, we leverage their favorable optical properties in a prototype UV imaging setup.

Introduction

Boron-containing luminescent molecules have gained attention for their application in areas such as OLEDs, (bio)sensing, and imaging.[1] These compounds normally consist of a boron atom nested in an aromatic organic framework, which interacts with the vacant p orbital of boron to produce charge transfer processes responsible for luminescence. Despite the abundance of hybrid (boron and carbon containing) luminescent molecules, only one boron hydride framework, *anti*-$B_{18}H_{22}$, exhibits fluorescence without the aid of any carbon-based functional groups. This 18-vertex borane has bright blue emission and a quantum yield nearing unity (ϕ = 0.97).[2] Since its discovery by Pitochelli and Hawthorne in 1962,[3] multiple follow-up investigations showed how functionalization of the boron vertices can have dramatic effects on its emission, quantum yield and stability.[4] With a limited number of synthetic derivatives reported to date, further work into defining the luminescent properties of B_{18}-based compounds *via* molecular design is needed. The recent research on *anti*-$B_{18}H_{22}$, led by Londesborough *et al.*, has so far focused on its application in lasers and OLEDs;[5] however, the lack of knowledge on its dynamic luminescent properties and UV stability- especially in polymer films- has so far thwarted such efforts.

This work considers the luminescence and UV stability of *anti*-$B_{18}H_{22}$-based molecules, with a focus on how and why these properties are subject to change in solution, neat powders, and polymer films. Specifically, we investigate *anti*-$B_{18}H_{22}$ (**1**) and two of its halogenated derivatives, 4,4'-Br_2-*anti*-$B_{18}H_{20}$ (**2**) and 4,4'-I_2-*anti*-$B_{18}H_{20}$ (**3**) (Figure 1). The parent borane **1** was selected to establish a baseline for these studies, while the halogenated clusters have luminescent properties favourable to optoelectronic application, such as absorption in the UV region, large Stokes' shifts, and high quantum yields.[4a] In this work, we show that the UV stability of **1**-**3** dramatically depends on the host matrix. Furthermore, we observe unique cage deconstruction chemistry that results in a loss of luminescence. Guided by this new knowledge, we were able to develop a

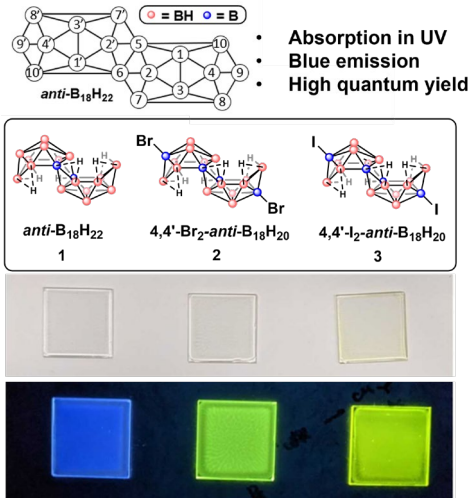

Fig. 1 Structures of the three luminescent compounds explored in this study (top) in polystyrene-toluene films under normal lighting (middle) and UV light (bottom).

[a] *Department of Chemistry and Biochemistry and California NanoSystems Institute (CNSI), University of California, Los Angeles, California 90095, USA*
[b] *Space Vehicles Directorate, Air Force Research Laboratory, Kirtland AFB, New Mexico 87117, USA*
[c] *Center for Micro-Engineered Materials, University of New Mexico, Albuquerque, New Mexico 87106, USA*
[d] *Department of Chemistry, University of California, San Diego, 9500 Gilman Drive, La Jolla, California 92093, USA*
[e] *USA Department of Chemistry, University of Southern California, Los Angeles, California 90089, USA*
[f] *BlueHalo, Albuquerque, New Mexico 87110, USA*
† *Footnotes relating to the title and/or authors should appear here.*
Electronic Supplementary Information (ESI) available: [details of any supplementary information available should be included here]. See DOI: 10.1039/x0xx00000x

proof-of-concept prototype UV-imaging setup using **1-3**. Importantly, this research identifies several interesting areas of *anti*-$B_{18}H_{22}$ chemistry that should be further addressed to achieve meaningful application of these clusters in optical devices.

Results and discussion

Incorporation of emitters into polymer films

Halogenated compounds **2** and **3** were selected for these studies due to their straightforward syntheses and large Stokes shifts that minimize reabsorption loss. While compound **3** has already been reported,[4a] its brominated counterpart, 4,4'-Br_2-*anti*-$B_{18}H_{20}$, is synthesized here for the first time. Substitution occurs via electrophilic halogenation by reacting *anti*-$B_{18}H_{22}$ with $AlCl_3$ and Br_2 over 1 hour (see SI, Figures S1-S5). All three compounds are stable when stored under ambient conditions. With **1**-**3** in hand, we sought suitable formulations for their incorporation into polymer films. Ideal films are uniform and should preserve the molecular photoluminescence and stability of the parent compound. However, embedding small molecules into polymer films can dramatically affect their properties. This, coupled with the poor solubility of inorganic emitters in organic solvents,[6] make developing and optimizing luminescent films extremely challenging. Previous studies demonstrated the ability to incorporate *anti*-$B_{18}H_{22}$ into polystyrene,[5] but only partial characterization of these films was conducted, and no other polymer matrices were explored. In this study, we investigate if and how the properties of **1**-**3** change when incorporated into four widely available and inexpensive polymers: poly(methyl methacrylate) (PMMA), poly(lauryl methacrylate) (PLMA), ethyl vinyl acetate copolymer (EVA), and polystyrene (PS). PMMA films loaded with 2 wt% **1**, **2**, and **3** were stable, but were also bright yellow in colour with significantly diminished luminescence when observed under a UV lamp (Figure S6). Both the PLMA and EVA films were colourless, but the emissive species degraded in the PLMA films after just 3 days and the EVA films were non-uniform and brittle. Only polystyrene yielded uniform, mostly colourless films that are stable under ambient conditions (Figure 1), making it the most suitable polymer matrix for the proceeding experiments.

Photoluminescent Characterization

Because molecular luminescence often changes when incorporated into films, photophysical characterization was conducted on cyclohexane solutions of **1**-**3** to establish baseline properties of each species. While the parent borane and its brominated analogue maintain absorption strictly within the UV region, 4,4'-I_2-*anti*-$B_{18}H_{20}$ tails slightly into the visible spectrum (Figure 2, left). Out of the three, **1** absorbs light most strongly (ε = 6800 $M^{-1}cm^{-1}$),[4b] followed by **3** (ε = 4900 $M^{-1}cm^{-1}$) and **2** (ε = 2200 $M^{-1}cm^{-1}$). Emission spectra, also gathered in cyclohexane solution, show peak maxima at 408, 525, and 526 nm for **1**, **2**, and **3**, respectively. The significant red-shifts in the emission spectra of **2** and **3** compared to the parent borane are due to the presence of the heavy halogen atoms, which lend spin-orbit coupling to the molecule. Previous reports have already noted that **1** exhibits fluorescence[2] and that the addition of heavy iodine atoms produces phosphorescence in **3**.[4a] Likewise, substitution with bromine results in phosphorescence, which occurs through a $^3(n_{Br} \rightarrow \sigma^*)$ charge transfer transition (Figure S43). Phosphorescence can be confirmed by the long 7 µs lifetime of **2**, which increases to 43 µs when nitrogen is bubbled through the solution (Figure S7). The quantum yields (ϕ) of the phosphorescent compounds improve under oxygen-free conditions, from ϕ = 0.08 to ϕ = 0.55 in **2** and from ϕ = 0.41 to ϕ = 0.71 in **3** (Table 1). We also note that **1**-**3** were stable in these solutions for at least several weeks, with no degradation observed.

Polystyrene films of these clusters, **PS-1**, **PS-2** and **PS-3**, were subjected to similar characterization, summarized in Table 1, Figures S8-S9, and Table S2. The optical properties of the films exhibit low reflectance and high transmittance (~90% at 500-2500 nm) with optical densities less than 1 for all three compounds (Figure S10). The absorption spectra remained largely unchanged from that of the cyclohexane solutions, while the emission peak maxima, particularly for **PS-1** and **PS-3**, exhibited noticeable bathochromic shifts of 25 nm and 10 nm, respectively (Figure 2, right). These shifts have been observed previously and are found to increase or decrease with higher and lower emitter loading, respectively; these changes could be caused by cluster-cluster or cluster-polymer interactions.[5b,7] The quantum yields also changed considerably from solution to films, with ϕ = 0.28 for **PS-1**, which is in stark contrast to the 0.97 value observed in cyclohexane solution.[2] Likewise, **3** exhibits a decrease from ϕ = 0.71 in solution[4a] to ϕ = 0.46 in film. Interestingly, only **PS-2** demonstrated improved quantum yield, increasing from ϕ = 0.41 to ϕ = 0.74 under nitrogen and exceeding the ϕ = 0.55 observed in oxygen-free cyclohexane. Diminished fluorescence of **1** in PS films was noted previously[5b] which the authors attributed to the high proton affinity (PA) of polystyrene that causes unfavourable interaction with the borane. They also reported that the quantum yield of PS films is negatively affected if they were cast with high PA solvents. Based on these findings, we prepared another batch of polystyrene films using dichloromethane which, in contrast to the previous report, exhibited slightly lower quantum yields than those cast with toluene (Table S2). Additionally, films cast with THF changed from yellow to opaque white upon drying, suggesting that the effects of the casting solvent are not well maintained in the dried films.

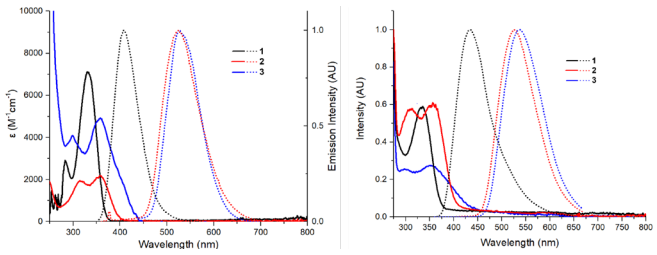

Fig. 2 Absorption and emission spectra of **1**-**3** in cyclohexane solution (left) and as 2 wt% polystyrene films (right), where the solid lines are absorption and the dotted lines are emission. λ_{exc} = 340 nm.

Table 1 Emission (λ_{em}), quantum yield (ϕ), lifetime (τ) and radiative ($k_r = \phi_{film}{}^{b}/\tau_{film}$) and non-radiative ($k_{nr} = (1-\phi_{film}{}^{b})/\tau_{film}$) decay rates for downshifting molecules. [a]In oxygen-free cyclohexane, [b]Under nitrogen atmosphere, [c]Under vacuum. [d]Data from PS films prepared with dichloromethane, see SI. Excitation wavelength (λ_{exc}) = 340 nm for emission and quantum yield, λ_{exc} = 331 nm for **1** and 405 nm for **2** and **3**. *From refs 2 and 4a.

	Anti-$B_{18}H_{22}$ (1)	4,4'-Br_2-*anti*-$B_{18}H_{20}$ (2)	4,4'-I_2-*anti*-$B_{18}H_{20}$ (3)
$\lambda_{em\ cyclohexane}$ (nm)	408	525	526
$\lambda_{em\ film}$ (nm)	434	526	538
$\phi_{cyclohexane}$	0.97*	0.55[a]	0.71[a]*
ϕ_{film}	0.28 0.30[b]	0.41 0.74[b]	0.44 0.46[b]
τ_{film} (μs)	0.0022[c,d]	58[c]	3.8[c]
k_r (μs^{-1})	86[d]	0.013	0.12
k_{nr} (μs^{-1})	370[d]	0.0045	0.14

To gain more specific insight into the conditions that quench luminescence, absorption and fluorescence spectra were gathered from solutions of **1-3** in cyclohexane, 1,2,-difluorobenzene, benzene, toluene, THF, acetone, and methanol (Figure S11-S13). The absorption maxima in each remain largely unchanged except for THF, acetone, and methanol, which show significantly (~60 nm) red-shifted peaks. Interestingly, 1,2-difluorobenzene also shifts the absorption of **2**. These changes are characteristic of a ground-state complex between the solvent and cluster forms that prevents luminescence.[8] To further investigate potential ground-state interactions between the borane and solvent molecules, **1**-**3** were analysed by ^{11}B and $^{1}H\{^{11}B\}$ NMR in deuterated THF, acetone, and methanol (Figures S14-23) and compared to their NMR spectra in deuterated chloroform solution. The effects of solvent on the ^{11}B NMR ranged from slight broadening of the boron resonances to wide, poorly defined peaks. For example, while the ^{11}B NMR spectrum of **1** in THF exhibits sharp boron resonances, the analogous spectrum in methanol is significantly broadened (Figures S14 and S16). These changes were often accompanied by increased number of resonances indicating decreased symmetry of the cluster. In several cases, sharp singlets indicative of tetracoordinate boron environments were observed (Figures S16-17, S22). Furthermore, broadening of the proton peaks in $^{1}H\{^{11}B\}$ NMR spectra points to the likelihood of exchange between solvent molecules and borane species. Interestingly, several proton resonances were completely absent in some methanol solution $^{1}H\{^{11}B\}$ NMR spectra, which is likely due to deuterium exchange between the cluster and solvent (Figure S16, S22). These data, in addition to the red-shifted absorption spectra (see above), strongly support the existence of ground-state complexes that prevent luminescence in coordinating solvents.

The minimal changes in the absorption spectra of compounds **1-3** in polystyrene and toluene suggest that the diminished quantum yield in these cases is due to a dynamic, excited-state process. Therefore, we conducted lifetime measurements in cyclohexane, 1,2-difluorobenzene, benzene, and toluene to investigate the variations in excited state dynamics in these solvents (Figure S24). The lifetime of **1** is longest in cyclohexane (10.4 ns) followed by 1,2-difluorobenzene (8.9 ns), toluene (4.8 ns), and benzene (3.3 ns). These successively shorter lifetimes, assuming monoexponential decay kinetics, signify stronger quenching caused by solvent. Interestingly, the decay kinetics of **1** in toluene are not monoexponential but are indicative of exciplex formation in the excited state.[8b] Propensity for toluene to strongly interact with **1** correlates to the severely diminished quantum yield observed in **PS-1**. In contrast to **1**, compound **2** exhibited the least amount of quenching from toluene, followed by benzene and 1,2-difluorobenzene (1,2-difluorobenzene also appears to form a ground-state complex with **2**). Notably, **3** only displays strong luminescence in cyclohexane and therefore the lifetime measurements in other solvents were not attempted.

These quenching mechanisms also manifest in polymer films: the less fluorescent yellow PMMA films likely indicate an interaction with the cluster that bears resemblance to that of the THF, methanol, and acetone solutions (Figure S6), while quenching by polystyrene could occur through excited state processes. **PS-2** and **PS-3** are less affected by the polymer matrix than **PS-1**, potentially because of the steric bulk of the substituents that mitigate cluster-polystyrene interactions, particularly in the solid state. At the same time, the progressively increasing polarizability from **1** to **3** could also render the halogenated molecules more susceptible to cluster-solvent interactions that diminish luminescence; it is therefore possible that **2** strikes a balance between these two quenching pathways that ultimately results in its superior quantum yield in polystyrene films. Still, while the exact quenching mechanisms cannot be definitively discerned from these studies, it is evident that quantum yield is dependent on the polymer host matrix, and it is essential that practitioners in future studies assess the intricate relationship between luminescence quenching by solvents and polymers.

Photostability of powders and polymer films

Data gathered for this report shows that polymers can greatly affect both the luminescence and stability of these boron clusters. We had previously identified two polymers, PMMA and PS, in which the clusters were stable under ambient conditions. However, we sought to gauge the extent of this stability under more relevant circumstances (i.e., light exposure). The photostability of **1** in polystyrene films has been previously investigated, with evidence of degradation observed after 30 minutes of light exposure, evidenced by diminished emission intensity.[5b] However, the degradation products of **1** are unknown and the photostability of **2** and **3** remain completely unexplored. Therefore, we conducted a more extensive study to assess the photostability of **1**-**3** as neat powders. To assess the degradation products of doped films, two different polymer hosts containing **1**-**3** were included in the study. Polystyrene and PMMA films as well as powders of **1**-**3** were subjected to intense UV irradiation over 7 days. All films

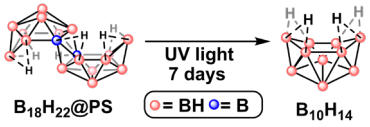

Fig. 3 Schematic of the deconstruction of **1** into its synthetic precursor, decaborane, after irradiation.

except **PMMA-1** exhibited decreased luminescence after light exposure. Each irradiated film was analysed by NMR spectroscopy and ESI-MS to identify the boron species present. Based on the NMR spectroscopy data, **PMMA-1** remained intact, while **PMMA-2** and **PMMA-3** showed little to no cluster present (Figure S25). Mass spectra for all three PMMA films dissolved in methanol show their respective boron cluster masses, indicating that at least some intact cluster remained (Figures S26-28). There was, however, no detectable intact cluster for **PS-1**, **PS-2**, and **PS-3** by NMR spectroscopy (Figure S29). The mass spectra showed no **1** or **2** present in the PS films, and only a small amount of **3** (Figures S30-32). We found the absence of detectable boron in these samples surprising; even if degradation had occurred, we would expect to see corresponding signals in the ^{11}B NMR spectra. To see if the boron content in the films was consistent before and after irradiation, Inductively Coupled Plasma – Optical Emission Spectrometry (ICP-OES) studies were conducted. Because the PMMA films were initially spin coated and the recovery of the PS films resulted in some lost fragments, we anticipated that the measured boron content would be slightly inaccurate or lower than the control samples. Nevertheless, the ICP results align well with the NMR and MS observations and show significantly less boron than expected (Tables S3-S4). In all films, the detected boron content was under 50% of the expected amount. In accordance with the MS and NMR spectroscopy data, the parent borane **1** performed best in the PMMA film, with 47% of the expected boron content present. The detected boron in the remaining PS and PMMA films was very low, apart from **PS-3** which had 32% remaining. Interestingly, a mass corresponding to $B_{10}H_{14}$ is present in the **PS-1** mass spectrum (Figure S33), suggesting that degradation could proceed through the deconstruction of the cluster cage into its synthetic precursor, decaborane.[10] To further probe this observation, irradiation of polystyrene films was conducted in sealed quartz tubes under ambient atmosphere. After irradiation, the contents of the quartz tubes were dissolved in deuterated chloroform for NMR analysis (Figure S34). The ^{11}B{^{1}H} NMR for **PS-1** contains several peaks that do not correspond to **1** but rather decaborane (Figure S35). At least another set of boron hydride peaks is clearly visible in the NMR spectrum which we were unable to definitively assign. There was no detectable boron by NMR spectroscopy for **PS-2** and **PS-3**. The mass spectra showed some intact cluster in **PS-1**, but most masses appeared to be degradation products, with one corresponding to decaborane ($B_{10}H_{14}$) (Figure S36). Interestingly, the MS of **PS-2** and **PS-3** did not contain the mass of $B_{10}H_{14}$, but rather its halogenated counterparts $B_{10}H_{13}Br$ and $B_{10}H_{13}I$, respectively (Figures S37-38). This suggests that degradation does not take place through cleavage of the boron-halogen bond, but through deconstruction of the B_{18}-based framework to form $B_{10}H_{14}$ (Figure 4). The relatively high vapor pressure of decaborane (0.2 mmHg)[11] explains its absence from the initial non-sealed samples, as it could easily escape the film after forming. Masses corresponding to other clusters, namely $B_{11}H_{14}^-$ and $B_{12}H_{16}O$, were also observed in the **PS-1** mass spectrum along with the corresponding halogenated masses for $B_{11}H_{13}X^-$, $B_{11}H_{13}XO^-$ and $B_{12}H_{15}XO$ in **PS-2** and **PS-3**. This suggests that cluster deconstruction proceeds through similar mechanisms for all three compounds tested. Despite the degradation observed in the films, the powder samples of compounds **1**, **2** and **3** were stable after the week-long irradiation (Figures S39-42). Evidence of intact **2** and **3** as well as $B_{18}H_{19}Br_3$ and $B_{18}H_{19}I_3$ by MS indicates that B-X bonds are less susceptible, but not inert, to photodegradation. Overall, these studies suggest that photostability of B_{18}-based compounds needs to be considered as a function of the host material.

UV-Visible imaging

Current UV-imaging technology is limited by its inability to simultaneously observe UV and visible light, mainly due to the opaque phosphors used.[12] With the appropriate setup,[13] our transparent, UV-absorbing films would permit the simultaneous visualization of UV and visible light. As a proof-of-concept to demonstrate the utility of compounds **1**-**3**, a prototype imaging setup was constructed using a 340 nm LED (Figure 4A). To ensure the purity of the LED, a 340 nm bandpass filter and focusing lens was placed in front of the light. A UV absorbing molecule, benzophenone, was dissolved in a solution of toluene and polystyrene and cast in a pattern ("UCLA") on a quartz substrate. The pattern is completely transparent and colourless, and it is not visible when placed in front of the bandpass filter in the presence of 340 nm light (Figure 4B, left). However, when polystyrene films of **1**-**3** are placed in front of the UV-absorbing pattern, the 340 nm light that is not absorbed by the benzophenone pattern is transmitted through the quartz and converted to a wavelength visible to the human eye or camera. Consequently, the UV absorber becomes visible (Figure 5B, right). One could further envision the incorporation of these emissive films onto the surface of camera lenses for the detection of UV radiation or UV absorbing objects, especially if better polymer formulations can be identified.

Conclusions

While *anti*-$B_{18}H_{22}$ and its derivatives remain a promising material for luminescence applications, the development of a suitable polymer formulation that yields transparent films, retains high quantum yield, and is stable to UV radiation is a

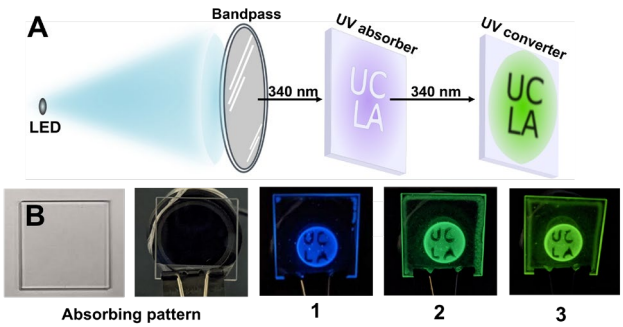

Fig. 4 A) Schematic of UV-imaging setup, viewed from the side B) Polystyrene films, from left to right: absorber film under ambient light, 340 nm light, the absorber film paired with emissive films **1**, **2**, and **3** under 340 nm illumination.

major bottleneck for their broader applications. This work provides a foundation for future studies by benchmarking dynamic photoluminescence and UV stability/degradation of B_{18}-based compounds as solids and in polymer films. We established that polymer matrices are intricately tied to luminescence and UV stability of the corresponding polymer films containing emissive boron clusters. The stability profile for these compounds under the same UV irradiation can be extreme, ranging from no noticeable degradation to nearly complete cage deconstruction. This study further serves as a broader reminder to practitioners in the field to carefully consider specific conditions and environmental factors when evaluating photostability of luminescent materials.

Author Contributions

We strongly encourage authors to include author contributions and recommend using CRediT for standardised contribution descriptions. Please refer to our general author guidelines for more information about authorship.

Conflicts of interest

There are no conflicts to declare.

Acknowledgements

A. M. S. acknowledges NSF Grants CHE-1846849 and DGE-1650604. We thank Boron Specialties for a gift of $B_{18}H_{22}$.

Notes and references

1 Recent representative examples: (a) Z. Huang, S. Wang, R. D. Dewhurst, N. V. Ignat'ev, M. Finze, H. Braunschweig, *Angew. Chem., Int. Ed.,* 2020, **59**, 8800-8816. (b) S. M. Berger and T. B. Marder, *Mater. Horiz.*, 2022, **9**, 112-120. (c) X. Su, T. A. Bartholome, J. R. Tidwell, A. Pujol, S. Yruegas, J. J. Martinez and C. D. Martin, *Chem. Rev.*, 2021, **121**, 4147-4192. (d) A. John, M. Bolte, H.-W. Lerner, G. Meng, S. Wang, T. Peng and M. Wagner, *J. Mater. Chem. C*, 2018, **6**, 10881-10887. (e) S. Mukherjee and P. Thilagar, *Chem. Commun.*, 2016, **52**, 1070-1093. (f) B. P. Dash, R. Satapathy, J. A. Maguire, N. S. Hosmane, *New. J. Chem.*, 2011, **35**, 1955-1972. (g) J. Ochi, K. Tanaka, Y. Chujo, *Angew. Chem., Int. Ed.*, 2020, **59**, 9841-9855. (h) K. O. Kirlikovali, J. C. Axtell, A. Gonzalez, A. C. Phung, S. I. Khan, A. M. Spokoyny, *Chem. Sci.*, 2016, **7**, 5132-5138. (i) X. Wu, J. Gu, Y. Quan, W. Jia, D. Jia, Y. Chen, Z. Xie, *J. Mater. Chem. C*, 2018, **6**, 4140-4149. (j) M. S. Messina, J. C. Axtell, Y. Wang, P. Chong, A. I. Wixtrom, K. O. Kirlikovali, B. M. Upton, B. M. Hunter, O. S. Shafaat, S. I. Khan, H. B. Gray, A. N. Alexandrova, H. D. Maynard, A. M. Spokoyny, *J. Am. Chem. Soc.,* 2016, **138**, 6952-6955. (k) P. Bissinger, A. Steffen, A. Vargas, R. D. Dewhurst, A. Damme, H. Braunschweig, *Angew. Chem., Int. Ed.,* 2015, **54**, 14, 4362-4366. (l) Y. Lebedev, C. Apte, S. Cheng, C. Lavigne, A. Lough, A. Aspuru-Guzik, D. S. Seferos, A. K. Yudin, *J. Am. Chem. Soc.* 2020, **142**, 13544-13549. (m) K. K. Hollister, A. Molino, G. Breiner, J. E. Walley, K. E. Wentz, A. M. Conley, D. A. Dickie, D. J.D. Wilson, R. J. Gilliard, *J. Am. Chem. Soc.,* 2022, **144**, 590-598. (n) L. Ji, S. Griesbeck, T. B. Marder, *Chem. Sci.*, 2017, **8**, 846-863. (o) J. Wang, N. Wang, G. Wu, S. Wang, X. Li, *Angew. Chem., Int. Ed.*, 2019, **58**, 3082-3086.

2 M. G. S. Londesborough, D. Hnyk, J. Bould, L. Serrano-Andrés, V. Sauri, J. M. Oliva, P. Kubát, T. Polívka and K. Lang, *Inorg. Chem*., 2012, **51**, 1471-1479.

3 A. R. Pitochelli and M. F. Hawthorne, *J. Am. Chem. Soc*., 1962, **84**, 3218-3218.

4 (a) M. G. S. Londesborough, J. Dolanský, J. Bould, J. Braborec, K. Kirakci, K. Lang, I. Císařová, P. Kubát, D. Roca-Sanjuán, A. Francés-Monerris, L. Slušná, E. Noskovičová and D. Lorenc, *Inorg. Chem.*, 2019, **58**, 10248-10259. (b) K. P. Anderson, M. A. Waddington, G. J. Balaich, J. M. Stauber, N. A. Bernier, J. R. Caram, P. I. Djurovich and A. M. Spokoyny, *Dalton Trans.*, 2020, **49**, 16245-16251. (c) M. G. S. Londesborough, J. Dolanský, T. Jelínek, J. D. Kennedy, I. Císařová, R. D. Kennedy, D. Roca-Sanjuán, A. Francés-Monerris, K. Lang and W. Clegg, *Dalton Trans.*, 2018, **47**, 1709-1725. (d) M. G. S. Londesborough, J. Dolanský, L. Cerdán, K. Lang, T. Jelínek, J. M. Oliva, D. Hnyk, D. Roca-Sanjuán, A. Francés-Monerris, J. Martinčík, M. Nikl and J. D. Kennedy, *Adv. Opt. Mater.*, 2017, **5**, 1600694. (e) V. Saurí, J. M. Oliva, D. Hnyk, J. Bould, J. Braborec, M. Merchán, P. Kubát, I. Císařová, K. Lang and M. G. S. Londesborough, *Inorg. Chem.*, 2013, **52**, 9266-9274.

5 (a) L. Cerdán, J. Braborec, I. Garcia-Moreno, A. Costela and M. G. S. Londesborough, *Nat. Commun.*, 2015, **6**, 5958. (b) J. Ševčík, P. Urbánek, B. Hanulíková, T. Čapková, M. Urbánek, J. Antoš, M. G. S. Londesborough, J. Bould, B. Ghasemi, L. Petřkovský and I. Kuřitka, *Materials*, 2021, **14**, 589. (c) J. Chen, L. Zhang, X. Huang, H. Meng, C. Tan, *Chem. Phys. Lett.*, 2020, **747**, 137328.

6 (a) M. Buffa, S. Carturan, M. G. Debije, A. Quaranta and G. Maggioni, *Sol. Energy Mater. Sol. Cells*, 2012, **103**, 114-118. (b) G. Griffini, *Front. Mater*., 2019, **6**.

7 E. J. M. Hamilton, R.G. Kultyshev, B. Du, E.A. Meyers, S. Liu, C.M. Hadad, S.G. Shore, *Eur. J. Chem.*, 2006, **12**, 2571.

8 (a) J. R. Lakowicz, *Principles of Fluorescence Spectroscopy*, Springer, Boston, MA, 3rd edn., 2006. (b) X. Poteau, A. I. Brown, R. G. Brown. C. Holmes, D. Matthew, *Dyes Pigm.* 2000, **47**, 91-105.

9 E. P. L. Hunter and S. G. Lias, *J. Phys. Chem. Ref. Data*, 1998, **27**, 413-656.

10 (a) B. M. Graybill, J. K. Ruff and M. F. Hawthorne, *J. Am. Chem. Soc.*, 1961, **83**, 2669-2670. (b) Y. Li and L. G. Sneddon, *Inorg. Chem.*, 2006, **45**, 470-471.

11 National Institute of Standards and Technology: *Decaborane(14)*, US Department of Commerce, Washington, DC, 2021.

12 W. A. R. Franks, M. J. Kiik, and A. Nathan, *IEEE Trans. Electron Devices*, 2003, **50**, 352-358.

13 J. Salman, M. K. Gangishetty, B. E. Rubio-Perez, D. Feng, A. Yu, Z. Yang, C. Wan, M. Frising, A. Shahsafi, and D. N. Congreve, *J. Opt.*, 2021, **23**, 054001.